

On the lack of thermal percolation in carbon nanotube composites

N. Shenogina, S. Shenogin, L. Xue, and P. Keblinski^{a)}

Department of Materials Science and Engineering, Rensselaer Polytechnic Institute, Troy, New York 12180-3590

(Received 14 March 2005; accepted 2 August 2005; published online 20 September 2005)

Recent experiments demonstrated very low percolation thresholds for carbon nanotube composites signified by steep increases in electrical conductivity at very low nanotube loadings. By contrast, thermal transport measurements, even on the same samples, showed no signature of the percolation threshold. These contrasting behaviors are particularly intriguing considering that both transport processes are described by the same continuum equation. In this letter we present a theoretical analysis based on finite element calculations that expose the underlying reasons for markedly different behaviors of electrical and thermal transport in high aspect ratio fiber composites. © 2005 American Institute of Physics. [DOI: 10.1063/1.2056591]

The issue of electrical conductivity of a composite consisting of conductive fillers dispersed in an insulating matrix is a classic percolation theory problem. The percolation theory,¹ validated by numerous experimental results,² predicts that a conductive network above, but near the percolation threshold, exhibits steep increases in electrical conductivity, σ , that obeys the universal power scaling law near the threshold

$$\sigma \sim (p - p_c)^\alpha, \quad (1)$$

where p is the filler volume fraction and p_c the volume fraction at the percolation threshold. The conductivity exponent $\alpha=2$ in three dimensions. This rapid conductivity increase is associated with (i) formation of the percolating cluster spanning the sample and (ii) attachment of isolated clusters to the percolating cluster and increased degree of connectivity within the percolating cluster. In practice, the crossing of the percolation threshold, within a narrow range of the conductive filler volume fraction, leads to an increase of several orders of magnitude in electrical conductivity.

In agreement with the percolation concept, recent experiments on carbon nanotube (CN) composites showed steep, “discontinuous” increases of electrical conductivity as the percolation threshold is crossed.³ Interestingly, measured percolation thresholds for CN composites are very low, of the order of 0.1 vol %, which can be compared with $p_c \sim 20\% - 30\%$ by volume, characterizing composites with spherical fillers. These low values of the percolation threshold originate from the fact that for random dispersion of fibers p_c is proportional to the inverse of the fiber aspect ratio.⁴ A simple dimensional analysis provides the estimate that the percolation threshold of 0.1% corresponds to the aspect ratio of about 300, with higher aspect ratios leading to lower p_c .

Surprisingly, thermal transport measurements on CN polymer composites and CN fluid suspensions show no signature of the percolation threshold. For example, Biercuk *et al.*⁵ showed that for single-walled CN-polymer composites, whereas the electrical transport shows a clear percolation threshold, the thermal conductivity is completely continuous at the threshold.

This markedly different behavior of electrical and thermal transport with respect to the development of the percolating network is quite puzzling considering that (i) electrical measurements show that the network is topologically percolating and (ii) the macroscopic descriptions of the electric and thermal current flows are described by the same equation.

In particular, for the steady state heat flow the temperature, T , satisfies the Laplace equation

$$\Delta T = 0 \quad (2)$$

with a requirement that at the filler-matrix interface the heat flux, J_Q , component normal to the interface is continuous

$$-J_Q = k_m \frac{\partial T_m}{\partial \mathbf{n}} = k_f \frac{\partial T_f}{\partial \mathbf{n}}, \quad (3)$$

where \mathbf{n} represents a coordinate normal to the interface, and k_m and k_f are thermal conductivities of the matrix and the filler, respectively. Equations describing the steady state flow of the electric current can be obtained simply by replacing the temperature by the voltage and the thermal by the electrical conductivities in Eqs. (2) and (3).

In this letter we demonstrate that the main reason for the difference between thermal and electrical transport responses to the onset of the percolating network in high aspect ratio composites is a relatively small thermal conductivity ratio k_f/k_m by comparison with the corresponding ratio of electrical conductivities. The secondary reasons are the contact resistance for the heat flow between fibers and the interfacial thermal resistance between fibers and the matrix.

To demonstrate our conjecture we performed the finite element method (FEM) based analysis of the key element of the network, namely a fiber-fiber contact. To model the contact we solved a steady state heat flow problem for two perpendicular cylindrical fibers with a diameter of 1.4 nm (which corresponds to a typical single-walled CN), embedded in a cylinder shaped calculation box filled with the matrix material, as shown in Fig. 1. The aspect ratio of the fibers in the model is about 300, and the height of the cylinder is about 200 times the fiber diameter. We varied surface-to-surface distance between fibers, h , from virtual contact to 100 nm. The ends of the “hot” fiber were kept at +50 °C, and the ends of the “cold” fiber at –50 °C. The adiabatic

^{a)}Electronic mail: keblip@rpi.edu

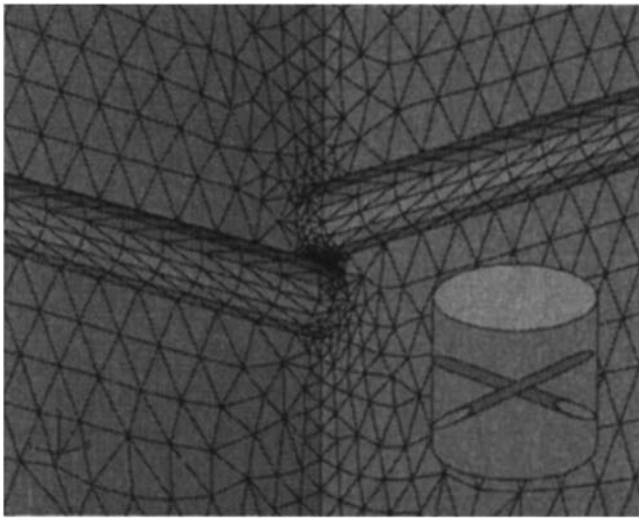


FIG. 1. A picture of the meshed model used in our FEM analysis. The inset shows two tubes crossed at 90° in a cylinder shaped calculation box. One tube's ends are held at $T=50^\circ\text{C}$, and the other tube's ends are at $T=-50^\circ\text{C}$. Due to the symmetry of this setup, only one quadrant of the system is considered in FEM calculations.

boundary conditions (i.e., zero normal thermal flux) were applied to the rest of the calculation box. Due to the symmetry of the problem, only one quadrant of the box was used for calculations (see Fig. 1).

The FEM analysis was performed using the commercial package ABAQUS. The FEM mesh consists of DC3D4 four-node tetrahedral elements. The total number of elements in the mesh representing the matrix and two CNs are about 174 000 and 15 000, respectively. Fine element sizes were assigned to important regions of fiber-matrix and fiber-fiber contact, while coarser mesh was used in other regions of the model. We also performed a sensitivity analysis, where the element length was decreased by a factor of 3 in the fiber-matrix contact region and by a factor of 10 in the fiber-fiber contact region. The maximum difference of 0.5% between the predicted temperatures was observed in the most critical region of the fiber-fiber contact.

We studied two models, the first employing the temperature continuity condition at the tube-matrix interfaces in addition to the flux continuity condition [Eq. (3)]. Such a model represents an interface of zero thermal resistance. In the second model, surface elements were used to represent interfacial thermal resistance between the fiber and the matrix. The value of this resistance has been measured recently for single-walled CNs in experiment,⁶ as well as calculated from the results of molecular dynamics simulations.^{6,7}

In our calculations we selected the conductivity of the fiber, $k_f=3000\text{ W/m K}$, which represents a value characteristic of carbon nanotubes.^{8,9} The selected matrix conductivity, k_m , is 0.138 W/m K and corresponds to the thermal conductivity of the oil used in a recent experiment on multi-walled carbon nanotubes suspensions.¹⁰ With these parameters the ratio k_f/k_m is of the order of 10^4 , which is characteristic of a typical carbon nanotube—low conductivity organic matrix composite. The fiber-matrix interfacial conductance value K (the inverse of the interfacial resistance) is $1.38 \times 10^7\text{ W/m}^2\text{ K}$ which corresponds to matrix thickness, $l_{eq}=10\text{ nm}$, over which, in planar geometry, the temperature drop is the same as at the interface ($l_{eq}=k_m/K$).⁶

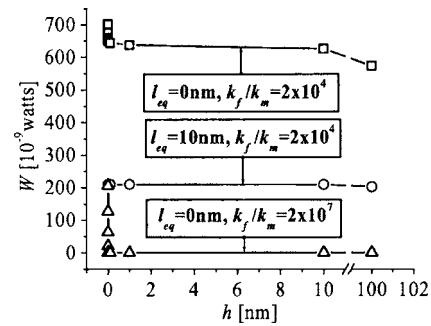


FIG. 2. The rate of heat flow, W , between nanotubes as a function of surface-to-surface separation. From the top to the bottom: (i) zero interfacial resistance, $k_f/k_m=2 \times 10^4$, (ii) interfacial resistance corresponding to $l_{eq}=10\text{ nm}$ of the material resistance, $k_f/k_m=2 \times 10^4$, (iii) zero interfacial resistance, $k_f/k_m=2 \times 10^7$.

Figure 2 shows the rate of the heat flow, W , from the hot to the cold fiber as a function of surface-to-surface separation, h . Quite remarkably, the variation of W with h is weak. For the zero interfacial resistance case there is a spike on the flux at the contact, but the magnitude of this spike is only several percent of the overall rate of the heat flow. This can only lead to a very minor percolation effect. The interfacial thermal resistance completely eliminates the contact signature in the heat flow between the fibers (see Fig. 2). In fact, for tube separations up to $\sim 10\text{ nm}$ the rate of heat flow is essentially constant, indicating that thermal fields associated with fibers are to a large extent shielded by the interface. In addition, the interfacial resistance significantly reduces the overall rate of the heat flow (see Fig. 2).

To gain a deeper understanding of the results presented in Fig. 2, in Fig. 3 we show the local temperature profiles along the straight lines on the surface of the hot tubes, on the side nearest to the cold tubes. For the tube with no interfacial resistance there is a significant temperature decrease from 50°C at the tube end towards the contact area. This decrease is associated with the heat dissipation into the matrix. This decrease is affected by the tube separation and for tubes in contact there is a sharp temperature drop in the contact area associated with large thermal fluxes. While this sharp drop results from the solution of the Laplace equation, it is not physical since it occurs over distances much shorter than the phonon free path, where the application of the diffusive equation of the heat flow is invalid. This problem indicates the limitation of the FEM method for describing the role of nanoscale features on thermal transport. However, for our system, large unphysical fluxes are limited to a small contact

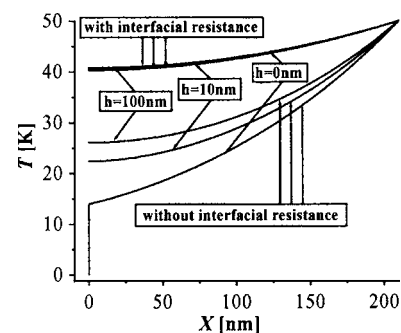


FIG. 3. The temperature along the straight line on the tube surface, on the side nearest to the other tube. $X=0$ corresponds to a point of the line at the center cross section of the tube.

area and, in consequence, their effect on the overall heat flow is small (see Fig. 2). Furthermore, in the case of real tubes the contact resistance would eliminate the high temperature gradient at the contact, again rendering the heat transport via contact not significant (see later discussion of molecular dynamics simulations).

For the tube with interfacial resistance the decrease of the temperature along the tube is much weaker since the heat dissipation to the matrix is diminished. In fact, the temperature profiles for tubes in contact and at 10 nm separation are indistinguishable. This is a manifestation of the thermal shielding due to interfacial thermal resistance. At larger separations (100 nm) there is change of the temperature profile, however very small. This weak temperature profile dependence on the tube separation is consistent with the almost separation independent rate of heat flow shown in Fig. 2.

In our analysis for the model with interfacial resistance we do not consider a direct heat flow from one tube to the other that “bypasses” interfacial resistance when tubes are in contact. By performing molecular dynamics simulations of the heat flow between X-crossed tubes interacting with each other via Van der Waals forces, we assessed that this channel of the heat flow is very ineffective. In fact, we found that the tube-tube contact conductance per unit area is about the same as the conductance of the tube-matrix interface. Considering that the contact area is very small, this heat channel can be neglected. Of course, with covalent bonding between the tubes the direct tube-tube heat flow would be significant, however, no such bonding is present in CN polymer composites or liquid suspensions. It is interesting to note that incorporation of the tube-tube contact resistance into our FEM analysis eliminates unphysically high temperature gradient in the contact area.

Let us now turn our discussion to the electrical percolation issue. The key difference between thermal and electrical transport is the value of the conductivity ratio. For the thermal problem, even for very conductive CNs, k_f/k_m is about 10^4 , while for the electrical transport, the ratio of conductivities can be of the order of 10^{12} – 10^{16} . With such high ratios, the only effective channel for the electric transport is along the percolating tube network. By contrast, in the thermal energy flow in CN composites the dominant channels of the heat flow always involve the matrix.

To illustrate the above discussion, in Fig. 2 we show the rate of thermal energy flow between two carbon nanotubes in a very low conductivity matrix as a function of tube separation. As in the first model studied, we consider tubes with no interfacial resistance, but we reduced thermal conductivity of the matrix by 1000 times leading to $k_f/k_m \sim 10^7$. According to Fig. 2, with this high ratio of conductivities there is very little heat flow between tubes, until tubes are in contact. At contact the heat flux increases by two orders of magnitude. Even sharper relative increases are expected for larger conductivity ratios. This will clearly lead to a strong percolation threshold in conductive transport. By contrast the actual ther-

mal conductivity ratio of $k_f/k_m \sim 10^4$ is just not high enough to induce a strong percolation threshold effect on thermal transport. Furthermore, with interfacial and contact thermal resistance the effects of percolation on thermal transport are completely eliminated.

Finally, we comment on the shape of experimentally observed thermal conductivity versus tube volume fraction curves. In an experiment on tubes in oil suspensions a significant nonlinear behavior was observed at very low volume fraction, with the conductivity-volume fraction curve exhibiting a positive curvature.¹⁰ By contrast, thermal transport measurements of water nanotube suspensions lead to a conductivity-volume fraction curve with a negative curvature.¹¹ Unlike both of these results, the effective medium theory, with or without interfacial resistance, predicts essentially linear conductivity-volume fraction curves at low volume fractions.¹²

Considering that the effective medium theory does not include the effects of interactions between thermal fields induced by the fibers, one might associate nonlinear behavior with those interactions. It is plausible that in the experiments yielding a positive curvature conductivity-volume fraction curve, interfacial resistance was relatively small, leading to additional increases of the thermal energy transport due to fiber contacts. We note that the contact density increases with the volume fraction square.¹³ A negative curvature in the conductivity-volume fraction curve might be associated with a large interfacial thermal resistance, which diminishes, rather than enhances, heat flow with increasing tube volume fraction.

This work was supported by DOE Grant No. DE-FG02-04ER46104 and the NSF Grant No. DMR 134725

¹D. Stauffer and A. Aharony, *Introduction to Percolation Theory* (Taylor & Francis, London, 1992).

²See, e.g., M. Sahimi, *Applications of Percolation Theory* (Taylor & Francis, London, 1994).

³J.-M. Benoit, B. Corraze, S. Lefrant, P. Bernier, and O. Chauvet, *Mater. Res. Soc. Symp. Proc.* **706**, Z3.28.1 (2002).

⁴I. Balberg, C. H. Anderson, S. Alexander, and N. Wagner, *Phys. Rev. B* **30**, 3933 (1984).

⁵M. J. Biercuk, M. C. Llaguno, M. Radosavljevic, J. K. Hyun, A. T. Johnson, and J. E. Fischer, *Appl. Phys. Lett.* **80**, 2767 (2002).

⁶S. Huxtable, D. Cahill, S. Shenogin, L. Xue, R. Ozisik, P. Barone, M. Usrey, M. Strano, G. Siddons, M. Shim, and P. Keblinski, *Nat. Mater.* **2**, 731 (2003).

⁷S. Shenogin, L. Xue, R. Ozisik, D. Cahill, and P. Keblinski, *J. Appl. Phys.* **95**, 6082 (2004).

⁸P. Kim, L. Shi, A. Majumdar, and P. L. McEuen, *Phys. Rev. Lett.* **87**, 215502 (2001).

⁹S. Berber, Y.-K. Kwon, and D. Tománek, *Phys. Rev. Lett.* **84**, 4613 (2000).

¹⁰S. U. S. Choi, Z. G. Zhang, W. Yu, F. E. Lockwood, and E. A. Grulke, *Appl. Phys. Lett.* **79**, 2252 (2001).

¹¹D. S. Wen and Y. L. Ding, *J. Thermophys. Heat Transfer* **18**, 481 (2004).

¹²C. W. Nan, R. Birringer, D. R. Clarke, and H. Gleiter, *J. Appl. Phys.* **81**, 6692 (1997).

¹³P. Keblinski and F. Cleri, *Phys. Rev. B* **69**, 184201 (2004).